Axion Emission from Strange Matter in Core-Collapse SNe

Maël Cavan-Piton,[1,*] Diego Guadagnoli,[1,†] Micaela Oertel,[2,‡] Hyeonseok Seong,[3,§] and Ludovico Vittorio[1,‖]
[1]LAPTh, Université Savoie Mont-Blanc et CNRS, 74941 Annecy, France
[2]Laboratoire Univers et Théories, Observatoire de Paris, Université PSL, CNRS, Université de Paris-Cité, 92190 Meudon, France
[3]Deutsches Elektronen-Synchrotron DESY, Notkestr. 85, 22607 Hamburg, Germany

(Received 22 February 2024; revised 29 May 2024; accepted 2 August 2024; published 17 September 2024)

The duration of the neutrino burst from the supernova event SN 1987A is known to be sensitive to exotic sources of cooling, such as axions radiated from the dense and hot hadronic matter thought to constitute the inner core of the supernova. We perform the first quantitative study of the role of hadronic matter beyond the first generation——in particular strange matter. We do so by consistently including the full baryon and meson octets, and computing axion emissivity induced from baryon-meson to baryon-axion scatterings as well as from baryon decays. We consider a range of supernova thermodynamic conditions, as well as equation-of-state models with different strangeness content. We obtain the first bound on the axial axion-strange-strange coupling, as well as the strongest existing bound on the axion-down-strange counterpart. Our bound on the latter coupling can be as small as $O(10^{-2})$ for $f_a = 10^9$ GeV.

DOI: 10.1103/PhysRevLett.133.121002

Introduction—Axions are among the best motivated and at present most sought-after particles beyond the standard model (SM). Searches and predictions follow two streams of activity. The first concerns the "invisible" [1–4] QCD axion [5–8], whose mass m_a and decay constant f_a are related—the smaller m_a the feebler the axion's interaction strength with known matter. The second stream of activity is the more general framework of axionlike particles (ALPs), where m_a and f_a are considered as independent parameters, constrained mostly by data (for UV aspects, see [9,10]).

In the QCD-axion case already, couplings to matter are very model dependent and are constrained through a wide and growing array of laboratory [11,12], astrophysical [13–15], or cosmological [16] observables, as well as by theoretical considerations [17–20]. Among astrophysical observables, core-collapse supernovæ (SNe) such as SN 1987A stand out. Measurements of the neutrino burst associated with SN 1987A [21–26] match expectations [27,28], and this provides a strong constraint on non-standard sources of cooling such as free-streaming axions a coupled to nucleons [29–31]. This is usually quantified through $Q_a < Q_\nu$ [13,31], with Q denoting the power radiated in the given particle per unit volume, or emissivity. The understanding of the different processes contributing to Q_a has seen rapid progress over recent years. The most established bound comes from axion-strahlung in nucleon-nucleon scattering [32], although a reliable calculation is challenging (see discussion in Ref. [15]). One class of processes that has received particular attention are pion-nucleon reactions $\pi N \to N' a$, which may even be dominant [33–40]. A further process considered recently is $\Lambda \to n a$, see [41–43].

The physics of axion emission from SNe is, however, still far from established in numerous respects, among the others: the hydrodynamical modelling of the SN, consistently including axion emission at the dynamical level as well as possible departures from spherical symmetry, see, in particular, [34,44–46]; the question how in-medium effects impact the leading axion-emission processes; the possible role of axion interactions with matter components inside the SN volume *beyond* the first generation of matter. Our work aims to perform a benchmark calculation that quantitatively addresses this last aspect. To this end, we evaluate the contributions to axion emissivity from all processes of the kind $B_i M \to B_f a$, where $B_{i,f}$ and M denote octet baryons and mesons, respectively, as well as the decays $B_i \to B_f a$. Their effect is nontrivial for the following reason. These contributions correspond to over one hundred different reactions, each yielding a *positive*-definite contribution to the emissivity Q_a. (By this argument, any additional process not included in our calculation would only make our conclusions stronger.) This large

*Contact author: cavanpiton@lapth.cnrs.fr
†Contact author: diego.guadagnoli@lapth.cnrs.fr
‡Contact author: micaela.oertel@astro.unistra.fr
§Contact author: hyeonseok.seong@desy.de
‖Contact author: ludovico.vittorio@lapth.cnrs.fr

Published by the American Physical Society under the terms of the Creative Commons Attribution 4.0 International license. Further distribution of this work must maintain attribution to the author(s) and the published article's title, journal citation, and DOI. Funded by SCOAP³.

number of processes compensates for the suppressed densities of strange baryons relative to those of ordinary nucleons [47–52]. As a result, Q_a serves as a nontrivial probe of axion interactions with strange matter. Specifically, the constraint from SN 1987A introduces new correlations between flavor-diagonal axial couplings involving an axion and any of the u, d, s quarks. Besides, this constraint introduces a *new bound* on the magnitude of the flavor-violating counterpart. This bound spans $O(10^{-1}$–$10^{-2})$, the range being determined by a variation of the thermodynamic conditions inside the axion-emitting SN core within realistic domains. Our bound assumes $f_a = 10^9$ GeV, but can be scaled to a different f_a choice through a well-defined procedure detailed later. Our work is, to our knowledge, the first study of axion emission from beyond-first-generation matter in the consistent framework of an effective theory, in particular, including all the allowed processes mentioned above.

Setup—We strived to test in detail the robustness of our conclusions with respect to the two main modeling aspects inherent in the system we consider: on the one hand, the modeling of the SN volume affected by axion emission, and on the other, of the axion-hadron interactions responsible for axion emission. We discuss these two key aspects in turn.

Our SN-core modeling is based on the following guidelines. Assuming weak equilibrium for the interactions that involve the strange quark, and neglecting the presence of muons, the state of matter is characterized by three thermodynamic parameters, chosen usually as the temperature T, baryon number density n_B, and electron fraction $Y_e \equiv (n_{e^-} - n_{e^+})/n_B$. These parameters allow us to determine the abundances of all particles entering the equation of state [53,54]. These parameters are, in general, *local* within the SN volume, and their values are obtained by solving the hydrodynamic equations from energy-momentum, baryon and electronic lepton number conservation, coupled to neutrino transport; see, e.g., [55]. Inclusion of axion transport accordingly allows us to account consistently for energy and momentum loss through axion emission, as described, e.g., in [34,44–46]. We do not perform here such a full-fledged SN simulation. Instead, we assume homogeneous thermodynamic parameters within the SN axion sphere, in an approach similar to much of the literature on axion emission from SNe [56]. For the parameters, we choose sets of values that should be representative of realistic conditions: $T = \{30, 40\}$ MeV; $n_B = \{1, 1.5\} n_{\rm sat}$, with $n_{\rm sat} = 1.6 \times 10^{38}$ cm^{-3}. As the third thermodynamic parameter, we take the total baryonic e.m. charge fraction $Y_{Q_B} \equiv \sum_{i \in B} Q_i n_i / n_B = 0.3$. Bearing in mind that hadron number fractions are dominated by nucleons (any other hadron contributing at the percent level or less) $Y_{Q_B} = 0.3$ ensures $Y_p \simeq 0.3$, consistent with the value adopted in, e.g., [33]. We note that the emissivity varies strongly with temperature—higher temperatures yielding larger Q_a values. We consider $T = 30$ MeV as it complies with a standard choice in the literature, and it also provides somewhat more conservative bounds from Q_a with respect to a higher T value. The case $T = 40$ MeV is, in turn, useful to quantify the effect of temperature variation in a reasonable, yet large enough range.

On top of the above thermodynamic-parameter choices, we also consider two equation-of-state (EOS) models consistently containing the full baryonic octet, `DD2Y` [57], and `SFHoY` [58]. This choice is guided by the following arguments among the others: these models specifically predict different amounts of strangeness inside hot and dense matter; they are publicly available; they are compatible with astro- and nuclear-physics constraints [57,58]. Hence, calculating Q_a within these two models provides a direct way to establish how sensitively our conclusions depend on the assumed amount of strange matter in the SN core. The meson octet is treated as an ideal Bose gas with chemical potentials obtained from the EOS model. Including an interaction between mesons and baryons would slightly modify the particle fractions, but we expect this to have a negligible impact on our conclusions [59]. The e^- fraction is then obtained from the condition of charge neutrality $Y_{Q_B} + Y_{Q_M} + Y_e = 0$.

The two EOS models, applied on the T and the n_B values discussed above, represent our ensemble of thermodynamic conditions. Specifically, each of them translates into a set of values for the chemical potentials of charged and neutral octet baryons and mesons. This allows us to calculate the axion emissivity Q_a for all the baryon-meson reactions of the type $B_i M \to B_f a$, as well as the decays $B_i \to B_f a$. The possible processes are listed in the Supplemental Material [60]. The diagrams relevant to $B_i M \to B_f a$ are depicted in Fig. 1.

The second modeling aspect that we need to specify is that of the axion-hadron interactions. The latter may be obtained through the Noether procedure applied to the 3-flavor octet-mesonic as well as -baryonic chiral Lagrangians, augmented with an axion as elucidated in [68]. Denoting the octet-meson and octet-baryon fields as U and B, respectively, one gets

$$\mathcal{L}_{aUB} = \frac{\partial_\mu a}{f_a} \sum_{b=1}^{8} \left(x_L^b \mathcal{J}_L^{b\mu}(U, B) + x_R^b \mathcal{J}_R^{b\mu}(U, B) \right), \quad (1)$$

where $x_{L,R}^b(a) \equiv \mathrm{Tr}\left(\hat{\boldsymbol{k}}_{L,R}(a) \lambda^b\right)$ are the axion-hadron coupling strengths of each of the interaction currents $\mathcal{J}_{L,R}^{b\mu}$ (collected for completeness in the Supplemental Material [60]). As is to be expected, these strengths are functions of $\hat{\boldsymbol{k}}_{L,R}$, i.e., the fundamental axion-quark coupling matrices defined from the Lagrangian [69]

$$\mathcal{L}_{aqq} \equiv \frac{\partial_\mu a}{f_a} \left(\bar{q} \gamma_L^\mu \hat{\boldsymbol{k}}_L(a) q + \bar{q} \gamma_R^\mu \hat{\boldsymbol{k}}_R(a) q \right), \quad (2)$$

with $q = (u, d, s)^T$ and $\gamma_{L,R}^\mu = \gamma^\mu (1 \mp \gamma_5)/2$.

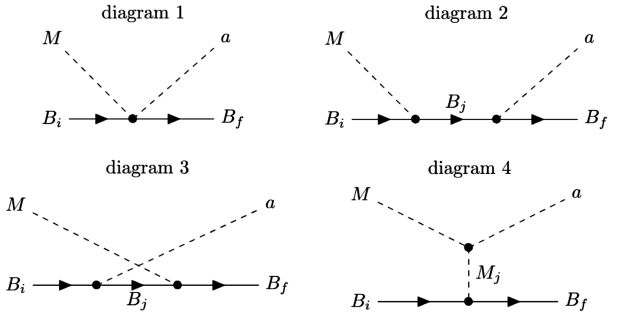


FIG. 1. The diagrams contributing to $B_i M \to B_f a$, with $B_{i,f}$ initial- or final-state octet baryons, M octet mesons, and a the axion.

As we consider processes involving a single axion, we can replace $\hat{\boldsymbol{k}}_{L,R}(a) \to \boldsymbol{k}_{L,R}$. Axion emissivity constrains the ratios $(\boldsymbol{k}_{L,R})_{ij}/f_a$, or equivalently, the $\boldsymbol{k}_{V,A} \equiv \boldsymbol{k}_R \pm \boldsymbol{k}_L$ counterparts. On the possible values for the indices, $ij = \{11, 22, 33, 23, 32\}$, we note the following. Hermiticity requires the diagonal entries to be real and the off-diagonal ones to have opposite phases; e.m. charge conservation sets to zero off-diagonal entries other than 23, 32. We have therefore a total of 10 parameters from $\boldsymbol{k}$ couplings, of which $(\boldsymbol{k}_{V,A})_{23}$ are genuine beyond-SM sources of strangeness-changing currents.

The $\boldsymbol{k}$ couplings are free parameters [68], fixed only by a theory of flavor, or by data. We stick to an agnostic approach, making no theoretical assumptions about any of the couplings. We sample them using uniform distributions over ranges covering several orders of magnitude and constrain them based on measurements. This ensures that the bounds we obtain are as conservative as possible. The entries $(\boldsymbol{k}_A)_{11}$ and $(\boldsymbol{k}_A)_{22}$ are bounded from data on isolated-neutron-star (NS) cooling, as recently discussed in Ref. [70]. To maintain our conservative stance, we have considered the scenario where axion couplings to neutrons and protons are both nonzero, and $\lesssim 10^{-9}$, which saturates the NS cooling bound. The couplings $(\boldsymbol{k}_{V,A})_{23}$ are generally constrained from kaon processes (henceforth "K bounds"), in particular $K^0 - \bar{K}^0$ mixing and $\Gamma(K \to \pi a)$. The latter process is sensitive to $|(\boldsymbol{k}_V)_{23}|$ alone, while the $K^0 - \bar{K}^0$-mixing constraint from the ϵ_K observable [71] jointly sets bounds on $(\boldsymbol{k}_V)_{23}$ and $(\boldsymbol{k}_A)_{23}$, see Ref. [41]. We compare the theoretical predictions against the $\Gamma(K \to \pi a)$ bound [72], as well as the 95% confidence-level range $0.88 < C_{\epsilon_K} < 1.36$ on $C_{\epsilon_K} \equiv |\epsilon_K^{\mathrm{SM}+a}|/|\epsilon_K^{\mathrm{SM}}|$, using the latest analysis by the UTfit Collaboration [73,74].

Some comments are in order on vectorial couplings. First, Q_a is insensitive to diagonal $\boldsymbol{k}_V$ couplings, which are solely observable via axion-hadron interactions whose underlying quark transition occurs via the weak force [68,69,76]. In addition, the Q_a bound on $|(\boldsymbol{k}_V)_{23}|$ is less stringent than the one from the nonobservation of $K \to \pi a$. Finally, the Q_a bound is also insensitive to the (difference between the) $(\boldsymbol{k}_V)_{23}$ and $(\boldsymbol{k}_A)_{23}$ phases.

Results—We next discuss our numerical results. We calculate the axion emissivity Q_a as [77]

$$Q_a = \int E_a (2\pi)^4 \delta^4(p) |\mathcal{M}|^2 \mathcal{F}_i \mathcal{F}_M (1 - \mathcal{F}_f) \times \prod_m^{\{i,f,M,a\}} \frac{d^3 \boldsymbol{p}_m}{(2\pi)^3 2E_m}, \tag{3}$$

where $|\mathcal{M}|^2$ denotes the absolute value squared of the amplitude $\sum_n \mathcal{A}(B_i M \to B_f a)$, $n = \{i, f, M\}$, where the indices i, f, M label the different possible instances of initial-, final-state baryon, and meson involved in the reactions. The distribution functions are defined as

$$\mathcal{F}_j = \frac{1}{\exp\left(\frac{E_j - \mu_j}{T}\right) + (-1)^{2s_j+1}}, \tag{4}$$

where s_j denotes the spin of the corresponding particle. Equation (3) generalizes to decays of the kind $B_i \to B_f a$ in an obvious way. As written, the emissivity treats all particles involved as ideal gases. However, in-medium effects in hot and dense matter are expected to have a strong impact [78,79]. Such effects may be captured at the mean-field level by shifting effective potentials, masses, and energies of all particles entering the EOS with their "effective" counterparts (e.g., Refs. [78–81]). Our case of more dilute matter is expected to yield weaker mean-field effects, but we leave the investigation of this issue to a separate study. We thus perform the replacements

$$m_j \to m_j^*, \quad E_j \to E_j^*, \quad \mu_j \to \mu_j^* = \mu_j - U_j, \tag{5}$$

where the right-hand side's are calculated within each of our considered thermodynamic conditions. In particular, the effective chemical potential contains the mean-field interaction potential U_j, which also enters the energy-conservation equation and is determined self-consistently. This treatment of mean-field effects also allows to correctly recover the particles' number densities by integrating their distribution functions over phase space.

We made two further validations. A first one was to employ the setup in Ref. [33]; namely, to restrict to the $\pi^- p \to n a$ process and further drop the first and fourth diagram in Fig. 1 (omitted in Ref. [33]) [82]. In such setup we find our results to be consistent with the predictions in Table I of Ref. [33]. A second check was to verify that the parameter bounds inferred from Q_a yield an axion mean free path [78] well above the SN radius, which validates the free-streaming assumption that underlies the Q_a calculation [13].

We are now ready to quantitatively discuss the implications of the bound $Q_a < Q_\nu$ [13,31] within the different

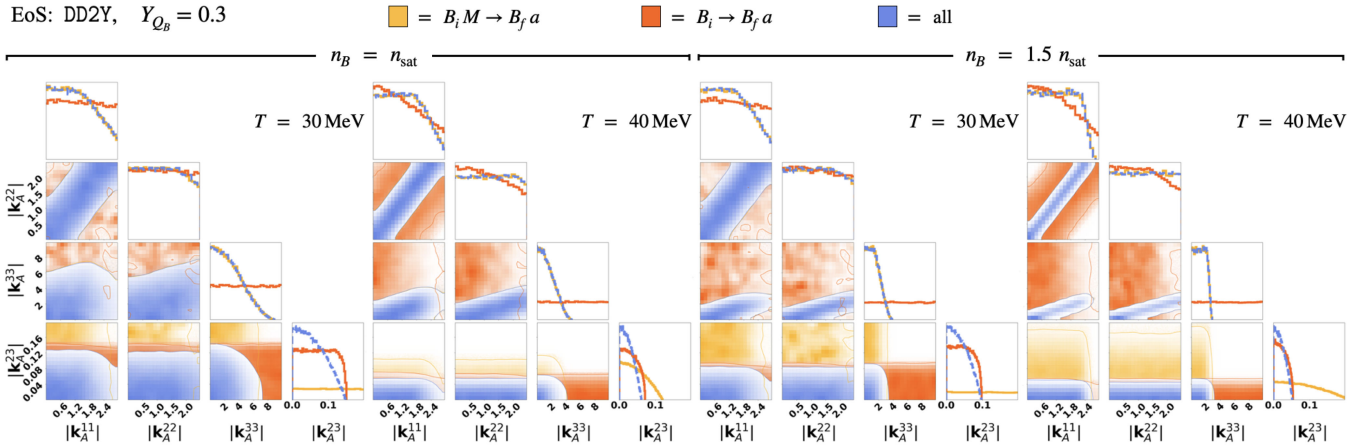


FIG. 2. Regions allowed to $|(\boldsymbol{k}_A)_{ij}|$, $ij = \{11, 22, 33, 23\}$ by $Q_a(B_i M \to B_f a)$ (yellow), $Q_a(B_i \to B_f a)$ (orange) and their sum (blue) $n_B = n_{\text{sat}}$ (first two panels) or $n_B = 1.5 n_{\text{sat}}$ (last two panels). The plots on the diagonal of each panel display the posterior distribution for the respective $\boldsymbol{k}$ coupling. The contour lines in the plots off-the-diagonal display marginalized 2D 95% posterior probabilities. The figure uses the DD2Y EOS with $Y_{Q_B} = 0.3$.

thermodynamic conditions and the different scenarios for the $\boldsymbol{k}$ couplings considered. The coherence of the results we obtain suggests the following general picture. Irrespective of the model, axion emissivity introduces nontrivial constraints on all of $|(\boldsymbol{k}_A)_{ij}|$, namely, $ij = \{11, 22, 33, 23\}$. In particular, (a) Q_a generates correlations between flavor-diagonal $\boldsymbol{k}_A$ couplings, due to its proportionality to the square of well-defined linear combinations of $(\boldsymbol{k}_A)_{ii}$ entries. Also, Q_a introduces a bound, albeit of $O(1)$ and thus mild, on all these entries; (b) Q_a introduces a novel, direct constraint on $|(\boldsymbol{k}_A)_{23}|$. The bound can be as low as 10^{-2} (for our reference f_a value), depending on the thermodynamic conditions chosen.

The above findings are illustrated in more detail in Fig. 2, which captures all the main messages of this study, but requires a detailed look. Each panel is a "matrix," showing the correlation of every parameter ($|(\boldsymbol{k}_A)_{11,22,33,23}|$ in the x axis) against every other one. The diagonal entries of the matrix are thus one-parameter histograms normalized to unity, where the remaining parameters are marginalized over, i.e., assumed to take on every possible value. The four instances of matrix plots in Fig. 2 refer to the two temperatures T and the two baryonic densities n_B considered, as specified in the legend. The three colors show the Q_a bound inferred from $B_i \to B_f a$ processes only (red), from $B_i M \to B_f a$ ones only (yellow), and from all (blue). The correlations [item (a)] are clearly visible as oblique blue bands; the bounds [item (b)] are the end points of the histograms along the diagonal of the matrix plots. As the lowermost histogram in each panel's diagonal shows, the $(\boldsymbol{k}_A)_{23}$ bound we obtain is highly nontrivial, and gets as low as 5×10^{-2} within the range of our considered thermodynamic conditions. The figure also suggests that (i) correlations become sharper and bounds tighter if T increases (first vs second, or third vs fourth panel); (ii) the bound on $(\boldsymbol{k}_A)_{33}$ is always dominated by $B_i M \to B_f a$ processes (yellow constraints); (iii) the bound on $(\boldsymbol{k}_A)_{23}$ is dominated by $B_i \to B_f a$ (red), although $B_i M \to B_f a$ processes (yellow) increase in importance for larger T. We also find that an increase in $n_B \in \{1, 1.5\} n_{\text{sat}}$ generally sharpens both findings (a) and (b). This is to be expected, as increasing n_B generally increases the hyperon phase space.

The largest possible values shown in the blue histograms (i.e., the histograms corresponding to Q_a calculated using all processes, $B_i M \to B_f a$ as well as $B_i \to B_f a$) on the diagonal of each panel of Fig. 2 are also tabulated in Table I. More precisely, they correspond to the large, boldfaced entries in this table, which refer to the DD2Y EOS model. The smaller entries on top of the large ones refer to the SFHoY EOS model instead, and are reported for direct comparison. This comparison shows at a glance that the DD2Y model leads to stronger bounds than SFHoY. Bounds are typically the result of several competing effects, and a numerical evaluation is necessary. For example, hyperon densities tend to be higher within DD2Y than they are in SFHoY (see also Supplemental Material [60]). On the other hand, for reactions involving hyperons as final state, smaller fractions are even advantageous.

We emphasize that, in both Fig. 2 and Table I, the $\boldsymbol{k}$ couplings are constrained solely by data, as described in the text between Eqs. (2) and (3). In other words, we make no model assumptions regarding the $\boldsymbol{k}$ couplings. It is useful to discuss how our obtained bounds would be modified if one imposes relations on the $\boldsymbol{k}$ couplings inferred from a theory of flavour. We mention two representative examples. A first one is the minimal QCD-axion solution to the flavor problem [83–88]. We find that Q_a is more constraining than the theory assumptions within this model, and our bounds in Table I remain valid.

TABLE I. Q_a bounds on $|(\boldsymbol{k}_A)_{23,33}|$, assuming $f_a = 10^9$ GeV. The larger boldfaced vs smaller value quoted in each table entry refers to the EOS model being considered, DD2Y [57] vs SFHoY [58] (see text for details on these models).

	$n_B = n_{\rm sat}$		$n_B = 1.5 n_{\rm sat}$	
$\boldsymbol{k}$ coupling	30 MeV	40 MeV	30 MeV	40 MeV
$\lvert(\boldsymbol{k}_A)_{23}\rvert$	0.35 **0.15**	0.12 **0.061**	0.38 **0.097**	0.14 **0.052**
$\lvert(\boldsymbol{k}_A)_{33}\rvert$	8.8 **8.9**	4.4 **4.8**	5.9 **3.9**	3.1 **2.9**

A second example is minimal flavor violation (MFV) [89–92] within axion models [93,94]. The minimal radiative flavor violation necessarily induces a very small left-handed off-diagonal component, scaling as $(\boldsymbol{k}_L)_{23} \sim (1/16\pi^2)(V_{\rm CKM})^*_{31}(V_{\rm CKM})_{32}$ multiplied by flavor-*universal* logs of ratios of ultraviolet scales. This functional dependence implies very suppressed values of $O(10^{-6})$. Besides, the right-handed counterpart is absent by definition. As a consequence $(\boldsymbol{k}_{V,A})_{23} \approx (\boldsymbol{k}_L)_{23} = O(10^{-6})$ or smaller within this scenario. In turn, the couplings $(\boldsymbol{k}_A)_{11,22,33}$ can be matched onto the axion-quark couplings $C_{u,d,s}$ of Refs. [35,95]. At a renormalization scale $\mu \approx 1$ GeV one has $C_{u,d,s} = O(10^{-2})$ within KSVZ models [1,2], and generically of $O(10^{-1})$ within DFSZ [3,4]. We thus see that, for any of the $\boldsymbol{k}$ couplings, Q_a is not constraining within this scenario, i.e., theory assumptions play a dominant role for all constrainable couplings.

We finally note that our results assume $f_a = 10^9$ GeV, which is the reference value throughout our numerical study. We decided to keep f_a fixed for two reasons. First, f_a can vary by orders of magnitude, and such variation would completely obliterate the Q_a dependence on $\boldsymbol{k}$ couplings, which are our focus. The question of what is the limit on f_a implied by our study necessarily requires to fix $\boldsymbol{k}_{11,22,33}$ and $|\boldsymbol{k}_{23}|$ first. Second, the Q_a dependence on f_a is ruled by a simple scaling: if $f_a \to f_a/x_f$, $Q_a \to Q_a x_f^2$.

In conclusion, we have presented the first study of SN axion emissivity Q_a that consistently quantifies the possible role of matter beyond the first generation, by calculating all baryon-meson to baryon-axion as well as baryon-decay processes involving the lightest baryon and meson octets. Q_a proves to be a strong constraint on axion interactions with strange matter. Specifically, we obtain the first bound on the axial axion-strange-strange coupling, and the strongest existing bound on the axion-down-strange counterpart. The latter spans the range $O(10^{-1}$–$10^{-2})$ depending on thermodynamic conditions chosen to realistically represent the SN axion-emitting core. Our study uses $f_a = 10^9$ GeV and $m_a \ll m_{B_i,B_f,M}$, i.e., it applies to the QCD axion, which is the most difficult to constrain. Our results suggest various additional applications, including to other compact objects and to axionlike particles with m_a comparable to the external states' masses. Importantly, we would like to further investigate the dependence of our results on the SN dynamics as well as on the EOS, in particular, the predicted particle abundances, along the lines discussed in the introduction. As a first step, one could test the effect of changing the interaction potentials that give rise to the different effective masses (and thus particle abundances), using justified ranges. The ultimate goal is, however, a full-fledged SN simulation that includes axion losses in the dynamics, similar to neutrino losses. This simulation should also allow for the exploration of the spatial dependence (radial, and beyond) of thermodynamical quantities, of the effects of different nuclear-matter EOS and of baryon-meson couplings. For the purely nucleonic case, see, e.g., Refs. [34,44–46].

Acknowledgments—We warmly thank Pierluca Carenza, Alessandro Lella, and Robert Ziegler for important feedback on their results. We also acknowledge useful discussions with Alexandre Carvunis and Kiwoon Choi. Finally, we are grateful to Yann Mambrini, Pierre Salati, and Guillaume Voisin for a critical reading of the manuscript. This work has received funding from the French ANR, under Contracts No. ANR-19-CE31-0016 (GammaRare), ANR-22-CE31-0001-01 (GW-HNS) and ANR-23-CE31-0018 (InvISYble), that we gratefully acknowledge. H. S. is supported by the Deutsche Forschungsgemeinschaft under Germany Excellence Strategy—EXC 2121 "Quantum Universe"—390833306.

[1] J. E. Kim, Weak interaction singlet and strong *CP* invariance, Phys. Rev. Lett. **43**, 103 (1979).
[2] M. A. Shifman, A. I. Vainshtein, and V. I. Zakharov, Can confinement ensure natural *CP* invariance of strong interactions?, Nucl. Phys. **B166**, 493 (1980).
[3] M. Dine, W. Fischler, and M. Srednicki, A simple solution to the strong *CP* problem with a harmless axion, Phys. Lett. **104B**, 199 (1981).
[4] A. R. Zhitnitsky, On possible suppression of the axion hadron interactions. (in Russian), Sov. J. Nucl. Phys. **31**, 260 (1980).
[5] R. D. Peccei and H. R. Quinn, *CP* conservation in the presence of instantons, Phys. Rev. Lett. **38**, 1440 (1977).
[6] R. D. Peccei and H. R. Quinn, Constraints imposed by *CP* conservation in the presence of instantons, Phys. Rev. D **16**, 1791 (1977).
[7] S. Weinberg, A new light boson?, Phys. Rev. Lett. **40**, 223 (1978).
[8] F. Wilczek, Problem of strong *P* and *T* invariance in the presence of instantons, Phys. Rev. Lett. **40**, 279 (1978).
[9] P. Svrcek and E. Witten, Axions in string theory, J. High Energy Phys. 06 (2006) 051.
[10] A. Arvanitaki, S. Dimopoulos, S. Dubovsky, N. Kaloper, and J. March-Russell, String axiverse, Phys. Rev. D **81**, 123530 (2010).

[11] I. G. Irastorza and J. Redondo, New experimental approaches in the search for axion-like particles, Prog. Part. Nucl. Phys. **102**, 89 (2018).

[12] P. Sikivie, Invisible axion search methods, Rev. Mod. Phys. **93**, 015004 (2021).

[13] G. G. Raffelt, Astrophysical methods to constrain axions and other novel particle phenomena, Phys. Rep. **198**, 1 (1990).

[14] G. G. Raffelt, Astrophysical axion bounds, Lect. Notes Phys. **741**, 51 (2008).

[15] A. Caputo and G. Raffelt, Astrophysical axion bounds: The 2024 edition, *Proc. Sci.*, COSMICWISPers (2024) 041 [arXiv:2401.13728].

[16] D. J. E. Marsh, Axion cosmology, Phys. Rep. **643**, 1 (2016).

[17] J. E. Kim and G. Carosi, Axions and the strong *CP* problem, Rev. Mod. Phys. **82**, 557 (2010); **91**, 049902(E) (2019).

[18] G. Grilli di Cortona, E. Hardy, J. Pardo Vega, and G. Villadoro, The QCD axion, precisely, J. High Energy Phys. 01 (2016) 034.

[19] L. Di Luzio, M. Giannotti, E. Nardi, and L. Visinelli, The landscape of QCD axion models, Phys. Rep. **870**, 1 (2020).

[20] K. Choi, S. H. Im, and C. Sub Shin, Recent progress in the physics of axions and axion-like particles, Annu. Rev. Nucl. Part. Sci. **71**, 225 (2021).

[21] R. M. Bionta *et al.*, Observation of a neutrino burst in coincidence with supernova SN 1987a in the Large Magellanic Cloud, Phys. Rev. Lett. **58**, 1494 (1987).

[22] C. B. Bratton *et al.* (IMB Collaboration), Angular distribution of events from Sn1987a, Phys. Rev. D **37**, 3361 (1988).

[23] K. Hirata *et al.* (Kamiokande-II Collaboration), Observation of a neutrino burst from the supernova SN 1987a, Phys. Rev. Lett. **58**, 1490 (1987).

[24] K. S. Hirata *et al.*, Observation in the Kamiokande-II detector of the neutrino burst from supernova SN 1987a, Phys. Rev. D **38**, 448 (1988).

[25] E. N. Alekseev, L. N. Alekseeva, V. I. Volchenko, and I. V. Krivosheina, Possible detection of a neutrino signal on 23 February 1987 at the Baksan Underground Scintillation Telescope of the Institute of Nuclear Research, JETP Lett. **45**, 589 (1987), http://jetpletters.ru/ps/index-v-45_en.shtml.

[26] E. N. Alekseev, L. N. Alekseeva, I. V. Krivosheina, and V. I. Volchenko, Detection of the neutrino signal from SN1987A in the LMC using the Inr Baksan Underground Scintillation Telescope, Phys. Lett. B **205**, 209 (1988).

[27] A. Burrows, Supernova explosions in the universe, Nature (London) **403**, 727 (2000).

[28] S. Woosley and T. Janka, The physics of core-collapse supernovae, Nat. Phys. **1**, 147 (2005).

[29] M. S. Turner, Axions from SN 1987a, Phys. Rev. Lett. **60**, 1797 (1988).

[30] G. Raffelt and D. Seckel, Bounds on exotic particle interactions from SN 1987a, Phys. Rev. Lett. **60**, 1793 (1988).

[31] A. Burrows, M. S. Turner, and R. P. Brinkmann, Axions and SN 1987a, Phys. Rev. D **39**, 1020 (1989).

[32] P. Carenza, T. Fischer, M. Giannotti, G. Guo, G. Martínez-Pinedo, and A. Mirizzi, Improved axion emissivity from a supernova via nucleon-nucleon bremsstrahlung, J. Cosmol. Astropart. Phys. 10 (2019). 016; 05 (2020) E01.

[33] P. Carenza, B. Fore, M. Giannotti, A. Mirizzi, and S. Reddy, Enhanced supernova axion emission and its implications, Phys. Rev. Lett. **126**, 071102 (2021).

[34] T. Fischer, P. Carenza, B. Fore, M. Giannotti, A. Mirizzi, and S. Reddy, Observable signatures of enhanced axion emission from protoneutron stars, Phys. Rev. D **104**, 103012 (2021).

[35] K. Choi, H. J. Kim, H. Seong, and C. S. Shin, Axion emission from supernova with axion-pion-nucleon contact interaction, J. High Energy Phys. 02 (2022) 143.

[36] B. Fore and S. Reddy, Pions in hot dense matter and their astrophysical implications, Phys. Rev. C **101**, 035809 (2020).

[37] A. Lella, P. Carenza, G. Lucente, M. Giannotti, and A. Mirizzi, Protoneutron stars as cosmic factories for massive axionlike particles, Phys. Rev. D **107**, 103017 (2023).

[38] S.-Y. Ho, J. Kim, P. Ko, and J. H. Park, Supernova axion emissivity with $\Delta(1232)$ resonance in heavy baryon chiral perturbation theory, Phys. Rev. D **107**, 075002 (2023).

[39] T. Vonk, F.-K. Guo, and Ulf-G. Meißner, Pion axioproduction: The Δ resonance contribution, Phys. Rev. D **105**, 054029 (2022).

[40] A. Lella, P. Carenza, G. Co', G. Lucente, M. Giannotti, A. Mirizzi, and T. Rauscher, Getting the most on supernova axions, Phys. Rev. D **109**, 023001 (2024).

[41] J. M. Camalich, M. Pospelov, Pham Ngoc Hoa Vuong, R. Ziegler, and J. Zupan, Quark flavor phenomenology of the QCD axion, Phys. Rev. D **102**, 015023 (2020).

[42] J. M. Camalich, J. Terol-Calvo, L. Tolos, and R. Ziegler, Supernova constraints on dark flavored sectors, Phys. Rev. D **103**, L121301 (2021).

[43] F. D'Eramo and S. Yun, Flavor violating axions in the early Universe, Phys. Rev. D **105**, 075002 (2022).

[44] K. Mori, T. Takiwaki, K. Kotake, and S. Horiuchi, Shock revival in core-collapse supernovae assisted by heavy axionlike particles, Phys. Rev. D **105**, 063009 (2022).

[45] A. Betranhandy and E. O'Connor, Neutrino driven explosions aided by axion cooling in multidimensional simulations of core-collapse supernovae, Phys. Rev. D **106**, 063019 (2022).

[46] K. Mori, T. Takiwaki, K. Kotake, and S. Horiuchi, Multimessenger signals of heavy axionlike particles in core-collapse supernovae: Two-dimensional simulations, Phys. Rev. D **108**, 063027 (2023).

[47] M. Oertel, F. Gulminelli, C. Providência, and A. R. Raduta, Hyperons in neutron stars and supernova cores, Eur. Phys. J. A **52**, 50 (2016).

[48] A. da Silva Schneider, E. O'Connor, E. Granqvist, A. Betranhandy, and S. M. Couch, Equation of state and progenitor dependence of stellar-mass black hole formation, Astrophys. J. **894**, 4 (2020).

[49] T. Malik, S. Banik, and D. Bandyopadhyay, New equation of state involving Bose-Einstein condensate of antikaon for supernova and neutron star merger simulations, Eur. Phys. J. Special Topics **230**, 561 (2021).

[50] H. Kochankovski, A. Ramos, and L. Tolos, Equation of state for hot hyperonic neutron star matter, Mon. Not. R. Astron. Soc. **517**, 507 (2022); **518**, 6376 (2022).

[51] A. R. Raduta, Equations of state for hot neutron stars-II. The role of exotic particle degrees of freedom, Eur. Phys. J. A **58**, 115 (2022).

[52] A. Sedrakian, J.-J. Li, and F. Weber, Heavy baryons in compact stars, Prog. Part. Nucl. Phys. **131**, 104041 (2023).

[53] H.-T. Janka, K. Langanke, A. Marek, G. Martinez-Pinedo, and B. Mueller, Theory of core-collapse supernovae, Phys. Rep. **442**, 38 (2007).

[54] M. Oertel, M. Hempel, T. Klähn, and S. Typel, Equations of state for supernovae and compact stars, Rev. Mod. Phys. **89**, 015007 (2017).

[55] S. W. Bruenn, Stellar core collapse: Numerical model and infall epoch, Astrophys. J. Suppl. Ser. **58**, 771 (1985).

[56] This picture—which builds on the fact that the main observable is the duration of the ν signal, whereas the amount of energy released is an inferred quantity—lends itself to the use of emissivity [13] to place the constraint, as we will discuss around Eq. (3).

[57] M. Marques, M. Oertel, M. Hempel, and J. Novak, New temperature dependent hyperonic equation of state: Application to rotating neutron star models and $I-Q$ relations, Phys. Rev. C **96**, 045806 (2017).

[58] M. Fortin, M. Oertel, and C. Providência, Hyperons in hot dense matter: What do the constraints tell us for equation of state?, Pub. Astron. Soc. Aust. **35**, 44 (2018).

[59] We note that the effect appears to be small at the temperatures of interest in our case [36].

[60] See Supplemental Material at http://link.aps.org/supplemental/10.1103/PhysRevLett.133.121002 for: a detailed list of allowed processes; explicit formulæ for axion-hadron interactions, also to fix notation; technical details on Fig. 2, and comparison plots within the SFHoY model; details on, and a listing of, SN particle fractions within our considered SN models. The Supplemental Material also makes reference to Refs. [61–67].

[61] S. Scherer, Introduction to chiral perturbation theory, Adv. Nucl. Phys. **27**, 277 (2003).

[62] T. Vonk, F.-K. Guo, and Ulf-G. Meißner, The axion-baryon coupling in SU(3) heavy baryon chiral perturbation theory, J. High Energy Phys. 08 (2021) 024.

[63] J. A. Cronin, Phenomenological model of strong and weak interactions in chiral $\mathrm{U}(3)\times\mathrm{U}(3)$, Phys. Rev. **161**, 1483 (1967).

[64] J. Kambor, J. H. Missimer, and D. Wyler, The chiral loop expansion of the nonleptonic weak interactions of mesons, Nucl. Phys. **B346**, 17 (1990).

[65] A. Notari, F. Rompineve, and G. Villadoro, Improved hot dark matter bound on the QCD axion, Phys. Rev. Lett. **131**, 011004 (2023).

[66] S. Typel, M. Oertel, and T. Klähn, CompOSE CompStar online supernova equations of state harmonising the concert of Nuclear Physics and astrophysics https://compose.obspm.fr, Phys. Part. Nucl. **46**, 633 (2015).

[67] S. Typel *et al.* (CompOSE Core Team), CompOSE reference manual, Eur. Phys. J. A **58**, 221 (2022).

[68] H. Georgi, D. B. Kaplan, and L. Randall, Manifesting the invisible axion at low-energies, Phys. Lett. **169B**, 73 (1986).

[69] M. Bauer, M. Neubert, S. Renner, M. Schnubel, and A. Thamm, Consistent treatment of axions in the weak chiral Lagrangian, Phys. Rev. Lett. **127**, 081803 (2021).

[70] M. Buschmann, C. Dessert, J. W. Foster, A. J. Long, and B. R. Safdi, Upper limit on the QCD axion mass from isolated neutron star cooling, Phys. Rev. Lett. **128**, 091102 (2022).

[71] R. L. Workman *et al.* (Particle Data Group), Review of particle physics, Prog. Theor. Exp. Phys. **2022**, 083C01 (2022).

[72] S. Adler *et al.* (E949, E787 Collaborations), Measurement of the $K^+\to\pi^+\nu\bar{\nu}$ branching ratio, Phys. Rev. D **77**, 052003 (2008).

[73] http://www.utfit.org/UTfit/

[74] We note that this range is only available on [73] as an online update, and is more recent that the latest published update in Ref. [75]. Our used range is nearly identical to the one used in Ref. [41].

[75] M. Bona *et al.*, Unitarity triangle global fits beyond the Standard Model: UTfit 2021 NP update, Proc. Sci. (EPS-HEP2021) 500.

[76] M. Bauer, M. Neubert, S. Renner, M. Schnubel, and A. Thamm, Flavor probes of axion-like particles, J. High Energy Phys. 09 (2022) 056.

[77] I. Tamborra, L. Hüdepohl, G. Raffelt, and H.-T. Janka, Flavor-dependent neutrino angular distribution in core-collapse supernovae, Astrophys. J. **839**, 132 (2017).

[78] G. Martinez-Pinedo, T. Fischer, A. Lohs, and L. Huther, Charged-current weak interaction processes in hot and dense matter and its impact on the spectra of neutrinos emitted from proto-neutron star cooling, Phys. Rev. Lett. **109**, 251104 (2012).

[79] L. F. Roberts, S. Reddy, and G. Shen, Medium modification of the charged current neutrino opacity and its implications, Phys. Rev. C **86**, 065803 (2012).

[80] S. Reddy, M. Prakash, and J. M. Lattimer, Neutrino interactions in hot and dense matter, Phys. Rev. D **58**, 013009 (1998).

[81] M. Oertel, A. Pascal, M. Mancini, and J. Novak, Improved neutrino-nucleon interactions in dense and hot matter for numerical simulations, Phys. Rev. C **102**, 035802 (2020).

[82] This comparison actually requires taking into account minor typos in Eqs. (5) and (11) of Ref. [33]. See also discussion in Ref. [37].

[83] Y. Ema, K. Hamaguchi, T. Moroi, and K. Nakayama, Flaxion: A minimal extension to solve puzzles in the standard model, J. High Energy Phys. 01 (2017) 096.

[84] L. Calibbi, F. Goertz, D. Redigolo, R. Ziegler, and J. Zupan, Minimal axion model from flavor, Phys. Rev. D **95**, 095009 (2017).

[85] D. B. Reiss, Can the family group be a global symmetry?, Phys. Lett. **115B**, 217 (1982).

[86] F. Wilczek, Axions and family symmetry breaking, Phys. Rev. Lett. **49**, 1549 (1982).

[87] Y. H. Ahn, Flavored Peccei-Quinn symmetry, Phys. Rev. D **91**, 056005 (2015).

[88] F. Björkeroth, E. J. Chun, and S. F. King, Accidental Peccei-Quinn symmetry from discrete flavour symmetry and Pati-Salam, Phys. Lett. B **777**, 428 (2018).

[89] R. S. Chivukula and H. Georgi, Composite technicolor standard model, Phys. Lett. B **188**, 99 (1987).

[90] L. J. Hall and L. Randall, Weak scale effective supersymmetry, Phys. Rev. Lett. **65**, 2939 (1990).

[91] G. D'Ambrosio, G. F. Giudice, G. Isidori, and A. Strumia, Minimal flavour violation: An effective field theory approach, Nucl. Phys. **B645**, 155 (2002).

[92] A. J. Buras, P. Gambino, M. Gorbahn, S. Jager, and L. Silvestrini, Universal unitarity triangle and physics beyond the standard model, Phys. Lett. B **500**, 161 (2001).

[93] K. Choi, S. H. Im, C. B. Park, and S. Yun, Minimal flavor violation with axion-like particles, J. High Energy Phys. 11 (2017) 070.

[94] F. Arias-Aragon and L. Merlo, The minimal flavour violating axion, J. High Energy Phys. 10 (2017) 168; 11 (2019) 152(E).

[95] K. Choi, S. H. Im, H. J. Kim, and H. Seong, Precision axion physics with running axion couplings, J. High Energy Phys. 08 (2021) 058.